JACC: CARDIOVASCULAR INTERVENTIONS VOL. 4, NO. 5, 2011

ISSN 1936-8798/$36.00
PUBLISHED BY ELSEVIER INC. DOI: 10.1016/j.jcin.2010.12.013

MINI-FOCUS ISSUE: PLAQUE COMPOSITION AND COMPLICATIONS
Clinical Research

Assessment of Echo-Attenuated Plaque by Optical Coherence Tomography and its Impact on Post-Procedural Creatine Kinase-Myocardial Band Elevation in Elective Stent Implantation

Tetsumin Lee, MD,* Tsunekazu Kakuta, MD,* Taishi Yonetsu, MD,* Kentaro Takahashi, MD,* Ginga Yamamoto, MD,* Yoshito Iesaka, MD,* Hideomi Fujiwara, MD,* Mitsuaki Isobe, MD†

Tsuchiura and Tokyo, Japan

Objectives This study examined morphological characteristics of echo-attenuated plaques by optical coherence tomography (OCT) and evaluated their influence on creatine kinase-myocardial band (CK-MB) elevation after percutaneous coronary intervention (PCI) in patients with elective stent implantation.

Background Recent intravascular ultrasound studies have described atherosclerotic plaques with echo attenuation (EA) without associated bright echoes that are correlated with no-reflow phenomenon after PCI.

Methods We studied 135 native de novo culprit coronary lesions in 135 patients with normal pre-PCI CK-MB levels (28 with unstable angina; 107 with stable angina) who underwent intravascular ultrasound and OCT examinations before elective stent implantation. The lesions were divided into 2 groups based on the presence or absence of EA, and OCT findings were compared. We then determined predictors of post-PCI CK-MB elevation.

Results EA was found in 47 (34.8%) lesions and was associated with the presence of OCT-derived thin-capped fibroatheroma, ruptured plaques, greater lipid content, intravascular ultrasound–derived large reference and plaque area, lesion eccentricity, and microcalcification. Elevated CK-MB levels were observed in 36 (26.7%) lesions, and significantly more frequently in lesions with EA than without. In multivariable analysis, EA (odds ratio [OR]: 3.49; 95% confidence interval [CI]: 1.53 to 7.93; $p = 0.003$) and OCT-derived ruptured plaque (OR: 2.92; 95% CI: 1.21 to 7.06; $p = 0.017$) were independent predictors of post-PCI CK-MB elevation.

Conclusions Atherosclerotic plaques with EA were associated with characteristics considered to be high risk or unstable. OCT examination showed an additive predictive value to the presence of EA for post-PCI CK-MB elevation. (J Am Coll Cardiol Intv 2011;4:483–91) © 2011 by the American College of Cardiology Foundation

From the *Department of Cardiology, Tsuchiura Kyodo Hospital, Tsuchiura, Japan; and the †Department of Cardiovascular Medicine, Tokyo Medical and Dental University, Tokyo, Japan. All authors have reported that they have no relationships to disclose.

Manuscript received August 16, 2010; revised manuscript received November 29, 2010, accepted December 9, 2010.

JACC: CARDIOVASCULAR INTERVENTIONS, VOL. 4, NO. 5, 2011
MAY 2011:483–91

Intravascular ultrasound (IVUS) can predict no-reflow or creatine kinase-myocardial band (CK-MB) elevation after percutaneous coronary intervention (PCI) based on characteristics such as a large plaque burden, intracoronary mobile mass, and lipid pool-like appearance (1–3). In addition, recent studies have described atherosclerotic plaques that show echo signal attenuation (EA) without associated bright echoes in patients with coronary artery disease, that is, associated with no-reflow and worse clinical outcome after PCI because of distal embolization (4–6). The ultrasound intensity of signal backscatter is affected by a number of factors, including tissue reflectivity and ultrasound power.

See page 492

Abbreviations and Acronyms

CK-MB = creatine kinase-myocardial band
CSA = cross-sectional area
EA = echo attenuation
EEM = external elastic membrane
IVUS = intravascular ultrasound
OCT = optical coherence tomography
PCI = percutaneous coronary intervention
SAP = stable angina pectoris
TCFA = thin-capped fibroatheroma
TIMI = Thrombosis In Myocardial Infarction
UAP = unstable angina pectoris

Coronary atherectomy specimens obtained from lesions with EA have shown the presence of predominantly lipid-rich plaque with microcalcification (4). However, very dense fibrous tissue may also produce EA (7). Lee et al. (5) reported that an echo-attenuated plaque is an exclusive marker of lesion instability observed only in patients with acute coronary syndrome, whereas others (4,6) detected a significant number of echo-attenuated plaques in stable lesions. Optical coherence tomography (OCT) is a high-resolution imaging method for plaque characterization providing information on plaque structures and tissue characterization, such as the presence of thin-capped fibroatheroma (TCFA), lipid-rich plaques, which are considered responsible for plaque instability, and intracoronary thrombi (8–12). Therefore, we hypothesized that OCT may allow us to elucidate the relevant morphological features of culprit coronary lesions with EA. To test this hypothesis, we evaluated plaques with and without EA by pre-PCI OCT examination in patients treated with elective stenting to investigate if lesions with EA are associated with OCT-derived high-risk plaque characteristics. We further hypothesized that OCT may allow us to detect lesion-related factors associated with post-PCI CK-MB elevation in these patients.

Methods

Study population. From December 2008 to December 2009, we prospectively enrolled 148 patients (32 with unstable angina pectoris [UAP] and 116 with stable angina pectoris [SAP]) without CK-MB elevation before PCI who underwent nonemergency stent implantation at single, native, de novo culprit coronary lesions at Tsuchiura Kyodo Hospital. Both IVUS and OCT examinations were performed before PCI. The study protocol was approved by the institutional review board, and all patients provided written informed consent before PCI. Patients treated with multivessel coronary intervention were excluded (1 UAP patient and 3 SAP patients). Patients were also excluded if they had significant left main disease (2 SAP patients), congestive heart failure, or renal insufficiency with baseline serum creatinine >1.8 mg/dl (133 μmol/l). In addition, those with extremely tortuous vessels or heavy calcification were excluded because of expected difficulty in advancing the OCT and/or IVUS catheters. We defined UAP as having a progressive crescendo pattern or angina at rest without an increase in troponin I. We defined SAP as no change in frequency, duration, or intensity of anginal symptoms within 6 weeks before PCI. The target lesion was identified by a combination of coronary angiograms, left ventricular wall motion abnormalities, electrocardiogram findings, angiographic lesion morphology, and scintigraphic defects. All included patients had angina, documented myocardial ischemia, or both. Three UAP patients and 4 SAP patients were further excluded from the analysis because of failure of the imaging catheter in crossing the lesion or unsatisfactory image quality. Thus, 28 UAP lesions and 107 SAP lesions from 135 patients were eventually analyzed in the present study. The presence of EA on IVUS was defined as an atherosclerotic plaque showing ultrasound signal attenuation without very high intensity echo reflectors that involved >90° of the vessel circumference and a length >1 mm. Lesions were divided into the group with EA in a culprit lesion (attenuated group) and the group without EA (nonattenuated group).

Percutaneous coronary intervention procedure. All patients received treatment with aspirin (200 mg/day) and clopidogrel (75 mg/day, 300-mg loading dose) at least 24 h before PCI. All patients received an intravenous bolus injection of 10,000 IU of heparin and intracoronary isosorbide dinitrate (2 mg) before angiography. PCI procedures were performed using a 6-F guiding catheter via the radial approach in all patients. Coronary stent implantation was performed with a balloon pre-dilation. Balloon/artery ratio for pre-dilation was 0.9 to 1.0 in all patients. To avoid aggressive stent expansion, stent size was guided by the combination of on-line quantitative coronary angiography and IVUS, although the type of stent was selected at the operator's discretion. Angiographic criteria of <25% residual stenosis were adopted as successful PCI. After achieving this endpoint, IVUS examination was performed to confirm optimal stent deployment and additional PCI was performed in case of a suboptimal result.

Quantitative coronary angiography analysis. Quantitative coronary angiography analysis was performed using a CMS-MEDIS system (Medis Medical Imaging Systems, Inc., Leiden, the Netherlands). The minimum lumen diameter, reference diameter, and lesion length were measured in diastolic frames from orthogonal projections. Coronary flow was assessed according to the Thrombolysis In Myocardial Infarction (TIMI) flow grade and corrected TIMI frame count (13,14).

CK-MB analysis. We took CK-MB measurements at the time of admission, within 1 h before PCI, 6 h and 20 h after PCI completion, and thereafter with an interval of 6 h if still continuing to increase. CK-MB activity was determined using an immunoinhibition assay and confirmed by mass assay technique. The maximum CK-MB value was considered to represent presence or absence of post-PCI CK-MB elevation. CK-MB elevation was defined as a level above the upper reference limit (URL) (16 IU/l).

OCT image acquisition and analysis. OCT image acquisition was performed using M3-CV and Image Wire 2 catheters (LightLab Imaging, Westford, Massachusetts) throughout the study. This system provides an axial resolution of 10 to 15 μm, lateral resolution of 20 to 40 μm, and 20 frames/s with 240 lines/frame. After obtaining control angiograms, the imaging wire was positioned distal to the region of interest with an occlusion balloon catheter (Herios, LightLab Imaging) located proximal to the lesion. If the lesion presented with tortuosity or severe stenosis and could not be crossed by the imaging catheter, we first advanced a conventional coronary guidewire (0.014 inch) across the lesion before replacing it with the OCT imaging wire over the balloon catheter. The lesions for which pre-dilation using a balloon was required to cross the OCT imaging wire were excluded. For clearing the operative field, the occlusion balloon was inflated to 0.5 atm, and Lactated Ringer's solution was continuously infused into the coronary artery through the distal tip of the occlusion catheter at 0.5 ml/s. The entire lesion's length was imaged with an automated pullback system at 1 mm/s. When a lesion was located close ($<$1 cm) to the ostium of the coronary arteries, we used the continuous-flushing nonocclusive technique for OCT imaging (15). To eliminate blood from the vessel without occlusion, we infused commercially available dextran-40 and Lactated Ringer's solution (Low molecular dextran L, Otsuka Pharmaceutical Factory, Tokushima, Japan) directly from the guiding catheter at a rate of 3.0 to 4.0 ml/s using a power injector (Angimat Illumena, Liebel-Flarsheim, Cincinnati, Ohio). Lesions with images showing significant signal attenuation but precluding satisfactory evaluation and reliable morphological measurement were excluded from the analysis. The image data were digitally stored for offline analysis. Using fluoroscopic reference and landmarks such as the aorto-ostial junction, proximal and distal side branches, and sites of calcification in combination with the constant pullback speed of the imaging wire and the OCT findings of each plaque, image location of all target sites could be determined and compared with IVUS findings. Offline analysis was performed with proprietary software (LightLab Imaging). The OCT data were analyzed by 2 independent investigators blinded to the angiographic and clinical findings using previously validated criteria for OCT plaque characterization (9,10,16). Discordance between investigators was resolved by consensus reading. The lipid content of a plaque was semiquantified as the number of involved quadrants on cross-sectional OCT images. For each plaque, the cross-sectional image with the highest number of lipid quadrants was used for further analysis. For all images of the culprit plaque with an OCT-determined lipid core, the overlying fibrous cap thickness was measured at its thinnest part. For each culprit plaque, the minimum value was used for subsequent analysis. When the number of lipid-containing quadrants was $\geq$2, it was considered as a lipid-rich plaque, whereas a TCFA was defined as a lipid-rich plaque with a fibrous cap thickness $<$70 μm. We also examined for fibrous cap disruption and an intracoronary thrombi. Fibrous cap disruption was identified by the presence of fibrous cap discontinuity and cavity formation in the plaque, and a plaque with fibrous cap disruption was defined as a ruptured plaque. In the ruptured plaque, the residual fibrous cap was identified as a flap between the lumen and the cavity of the plaque, and its thickness was measured at the thinnest part. Intracoronary thrombi were identified by mass images protruding into the lumen. Interobserver and intraobserver differences were assessed by evaluation by 2 observers and by 1 observer at 2 separate time points, respectively.

IVUS image acquisition and analysis. After OCT examination, IVUS imaging was attempted for all patients before any PCI procedure after intracoronary administration of 200 μg of nitroglycerin using a 40-MHz IVUS catheter (Boston Scientific, Natick, Massachusetts). The catheter was advanced distal ($>$10 mm) to the target lesion up to a distal landmark point documented by angiography. Automated pullback at 0.5 mm/s was then performed from this point to the aorto-ostial junction. IVUS images were digitally stored for subsequent offline analysis. Two independent investigators blinded to the angiographic, OCT, and other clinical data analyzed the IVUS images. Discordance between the observers was settled by consensus reading. Qualitative and quantitative IVUS analysis was performed according to the American College of Cardiology Clinical Expert Consensus Document (7). Lesion site was at the minimum lumen cross-sectional area (CSA). Using planimetry software (QCU-CMS, Medis Medical Imaging Systems, Inc.), external elastic membrane (EEM) and lumen CSAs were measured. Plaque plus media CSA was calculated as EEM minus

JACC: CARDIOVASCULAR INTERVENTIONS, VOL. 4, NO. 5, 2011
MAY 2011:483–91

lumen CSA, and plaque burden was calculated as plaque plus media divided by EEM CSA. If the EEM circumference could not be identified, we interpolated the EEM area. The location of the echo-attenuated portion of the plaque was documented for comparison with the OCT findings. Proximal and distal references were single slices with the larger lumen and smallest plaque burden within 10 mm proximally and distally, but occurring before any large side branch. The eccentricity was the ratio of maximum to minimum plaque thickness; lesions were characterized as concentric when the ratio was <2 and eccentric when the ratio was ≥ 2. The remodeling index was defined as the ratio of the lesion EEM CSA to the reference EEM CSA. Positive remodeling was defined as remodeling index of >1.05. Bright echoes with $<90^{\circ}$ of acoustic shadowing of a size <1 mm were defined as mild calcifications.

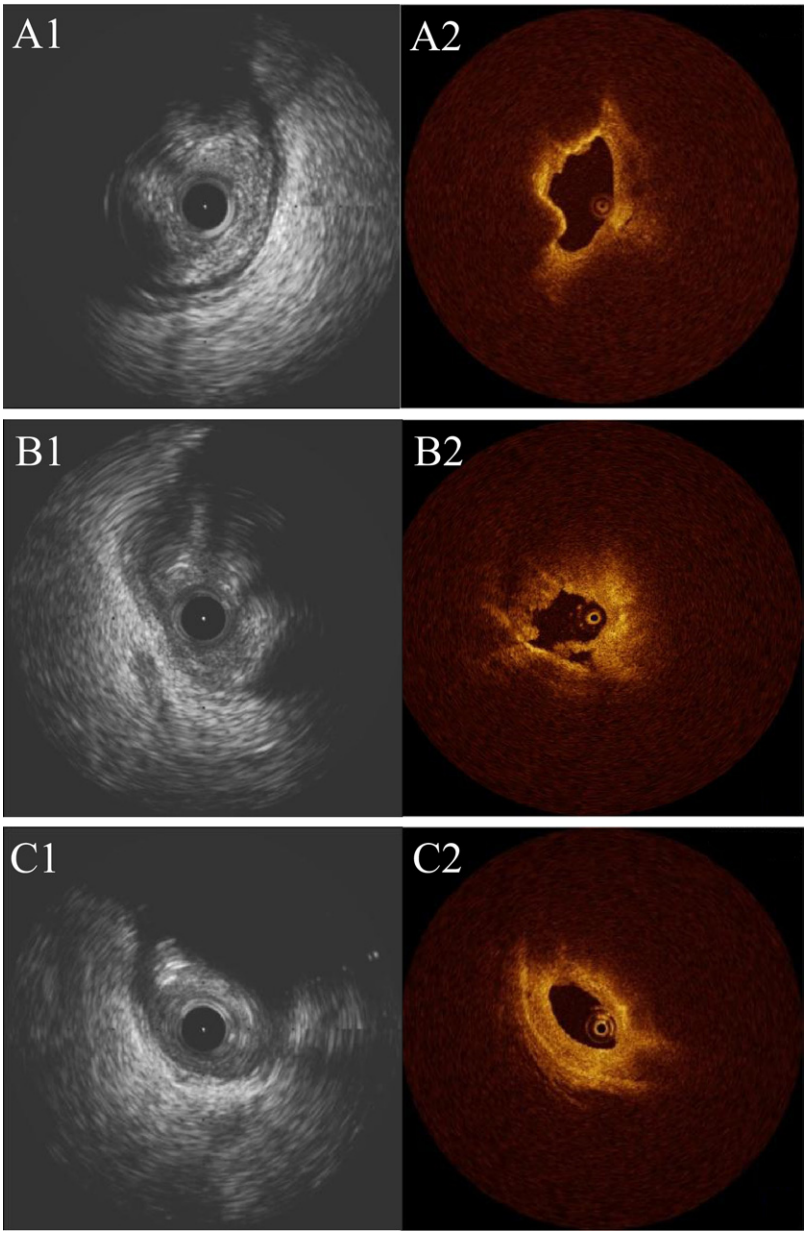

Figure 1. Echo-Attenuated Plaques and Corresponding OCT Images

Echo-attenuated plaques **(A1, B1, and C1)** and the corresponding optical coherence tomography (OCT) images **(A2, B2, and C2).** The OCT examination showed thin-capped fibroatheroma **(A2)** and large thrombus **(B2)** at the echo attenuation (EA) site. A lipid-rich plaque with a thick fibrous cap was detected on OCT at the EA site **(C2)**.

Statistical analysis. SPSS (version 14.0, SPSS, Inc., Chicago, Illinois) was used for all analyses. Categorical data were expressed as absolute frequencies and percentages and were compared using the chi-square or Fisher exact tests, as appropriate. Continuous variables were expressed as mean ± SD for normally distributed variables and as median (25th to 75th percentile) for not normally distributed variables; they were compared using Student *t* test and Mann-Whitney *U* tests, respectively. Interobserver and intraobserver variabilities of IVUS and OCT findings were assessed by the kappa statistic of concordance. Trend tests were performed to test the relationship between OCT-derived characteristics and peak CK-MB category. To control for multiple comparisons, pairwise tests were performed. The relationship between CK-MB elevation (dependent variable), the presence of EA, OCT findings, and other potential confounders were assessed using multivariable logistic regression analysis (stepwise forward method) to assess whether EA remained associated with CK-MB elevation. The associated variables in univariable analyses ($p < 0.2$) were included in the model. The Hosmer and Lemeshow test was used to establish the goodness-of-fit of the model. A p value of >0.05 indicates that the model provides a valid representation. We considered $p < 0.05$ to indicate statistical significance.

Results

IVUS and OCT images were available for analysis in 28 culprit lesions in 28 UAP patients and 107 culprit lesions in 107 SAP patients. Attenuated plaques were found in 47 lesions (34.8%): 6 of 28 (21.4%) in UAP; 41 of 107 (38.3%) in SAP; $p = 0.12$. Representative images are shown in Figure 1.

Patient characteristics, angiographic, and procedural results. There were no differences in age, sex, clinical presentation, and cardiovascular risk factors between the 2 groups (Table 1). Angiographic data (Table 2) showed that attenuated plaques were observed more frequently in the right coronary artery and less frequently in the left anterior descending coronary artery. In all patients, successful stenting was performed. Drug-eluting stents were used more often in patients from the nonattenuated group. Baseline TIMI flow grade and corrected TIMI frame count did not differ between the 2 groups. Immediately after balloon angioplasty and at final angiography, the TIMI flow grade and corrected TIMI frame count were both significantly worse in the attenuated group.

IVUS findings. Plaque burden, eccentricity index, lesion EEM, and reference EEM area values were significantly greater in the attenuated group, whereas the lesion lumen area was similar between the 2 groups (Table 3). Mild calcification was more frequently detected in the attenuated lesions than in nonattenuated lesions ($p = 0.01$). We observed EA at the minimal lumen CSA site in 45 lesions (95.7%), proximally in 1 lesion (2.1%), and distally in 1 lesion (2.1%).

Table 1. Patient Characteristics

	Attenuated Group (n = 47)	Nonattenuated Group (n = 88)	p Value
Age, yrs	67.0 ± 10.5	64.6 ± 10.2	0.20
Female	6 (12.8)	20 (22.7)	0.20
Diabetes mellitus	15 (31.9)	35 (39.8)	0.46
Hypertension	37 (78.7)	63 (71.6)	0.42
Current smoker	24 (51.1)	39 (44.3)	0.47
Previous MI	12 (25.5)	20 (22.7)	0.88
UAP	6 (12.8)	22 (25.0)	0.12
CRP, mg/dl	0.06 (0.00–0.25)	0.06 (0.00–0.52)	0.44
WBC, counts/μl	6,354 ± 1,469	6,404 ± 1,820	0.87
Total cholesterol, mg/dl	194 ± 36	198 ± 40	0.61
LDL cholesterol, mg/dl	122 ± 31	120 ± 33	0.76
HDL cholesterol, mg/dl	44 ± 14	45 ± 11	0.64
Peak CK-MB, IU/l	15 (10–20)	11 (9–15)	0.003
Statin use	26 (55.3)	43 (48.9)	0.59

Values are mean ± SD, n (%), or median (25th to 75th percentile).
CK-MB = creatine kinase-myocardial band; CRP = C-reactive protein; HDL = high-density lipoprotein; LDL = low-density lipoprotein; MI = myocardial infarction; UAP = unstable angina pectoris; WBC = white blood cell.

OCT findings. OCT revealed that the frequency of TCFA was significantly greater in the attenuated group than in the nonattenuated group (Table 4). The fibrous cap thickness of lipid-rich plaques in the attenuated group was significantly lesser than that in the nonattenuated group.

Predictors of post-PCI CK-MB elevation. Elevated post-PCI CK-MB levels were observed in 36 patients and more frequently in the attenuated group: in 21 lesions with EA (21 of 47, 44.7%) and 15 lesions without EA (15 of 88, 17.0%); $p = 0.001$. When lesions with elevated CK-MB levels were divided into 2 groups (≥3 × URL and >1 to 3 × URL), the frequencies of EA, TCFA, and ruptured plaques increased proportionally to the magnitude of CK-MB elevation levels (Fig. 2), whereas the frequency of thrombi was not statistically different among the groups (16.2%, 13.3%, and 33.3%, respectively, $p = 0.48$). Fibrous cap thickness was significantly thinner in the highest CK-MB elevation group (Fig. 3). When patients with plaque rupture (n = 32) were divided into 2 groups on the basis of EA, the peak CK-MB levels were significantly greater in the attenuated group with ruptured plaques (n = 16) than in the nonattenuated group with ruptured plaques (n = 16) (20 IU/l [interquartile range (IQR): 14 to 76 IU/l] vs. 13 IU/l [IQR: 8 to 18 IU/l], $p < 0.01$), whereas the frequency of post-PCI CK-MB elevation was not statistically different between the 2 groups (62.5% vs. 31.3%, $p = 0.16$). Multivariable analysis revealed that factors independently associated with post-PCI CK-MB were EA (OR: 3.49; 95% CI: 1.53 to 7.93; $p = 0.003$) and OCT-derived ruptured plaque (OR: 2.92; 95% CI: 1.21 to 7.06; p =

Table 2. Angiographic Findings

	Attenuated Group (n = 47)	Nonattenuated Group (n = 88)	p Value
Lesion location			0.001
RCA	28 (59.6)	31 (35.2)	
LAD	9 (19.1)	45 (51.1)	
LCX	10 (21.3)	12 (13.6)	
Pre-MLD, mm	1.06 ± 0.34	1.00 ± 0.37	0.32
Pre-RD, mm	3.21 ± 0.47	2.84 ± 0.57	<0.001
Stenosis, %	66.5 ± 10.9	64.7 ± 11.8	0.38
Lesion length, mm	15.3 (12.1–19.6)	13.5 (10.5–19.2)	0.28
ACC/AHA classification B2/C	28 (59.6)	41 (46.6)	0.21
Post-MLD, mm	3.29 ± 0.43	3.07 ± 0.43	0.004
Post-dilation pressure, atm	15.3 ± 2.5	15.9 ± 3.2	0.25
Stented length, mm	24 (20–32)	28 (23–35)	0.12
Acute gain, mm	2.21 ± 0.60	2.05 ± 0.48	0.11
Drug-eluting stents	31 (66.0)	74 (84.1)	0.028
TIMI flow grade			
Before procedure			0.22
0–1	1 (2.1)	1 (1.1)	
2	2 (4.3)	12 (13.6)	
3	44 (93.6)	75 (85.2)	
After balloon angioplasty			0.003
0–1	1 (2.1)	1 (1.1)	
2	16 (34.0)	9 (10.2)	
3	30 (63.8)	78 (88.6)	
At final angiogram			0.002
0–1	1 (2.1)	0 (0.0)	
2	7 (14.9)	1 (1.1)	
3	39 (83.0)	87 (98.9)	
CTFC			
Before procedure	25 (20–27)	24 (19–27)	0.66
After balloon angioplasty	27 (21–34)	20 (14–26)	<0.001
At final angiogram	21 (18–26)	18 (13–23)	0.006

Values are n (%), mean ± SD, or median (25th to 75th percentile).

ACC/AHA = American College of Cardiology/American Heart Association; CTFC = corrected TIMI frame count; LAD = left anterior descending; LCX = left circumflex; MLD = minimal lumen diameter; RCA = right coronary artery; RD = reference diameter; TIMI = Thrombolysis In Myocardial Infarction.

0.017) (Table 5). In attenuated plaques with plaque rupture, the OR of post-PCI CK-MB elevation increased to 5.96 (95% CI: 1.98 to 17.93; p = 0.001) as compared to lesions without these 2 characteristics. The Hosmer and Lemeshow test provided p values of 0.997, which indicated a proper goodness-of-fit for the model.

Intraobserver and interobserver variability. Intraobserver and interobserver variability of IVUS findings yielded good concordance for the presence of EA (kappa = 0.91 for intraobserver variability and kappa = 0.85 for interobserver variability). Intraobserver variability of OCT findings yielded high concordance, whereas interobserver variability showed slightly lower concordance for lipid quadrants (kappa = 0.90 vs. 0.83), identification of TCFA (kappa = 0.83 vs. 0.77), and thrombus (kappa = 0.92 vs. 0.84).

Discussion

Our major findings are as follows: 1) an attenuated plaque was found in 34.8% of the present cohort; 2) the minimum lumen site was located at the attenuated portion of the culprit plaque in the majority (95.7%) of lesions in the attenuated group; 3) the echo-attenuated plaque was associated with high-risk characteristics, such as large reference area, greater plaque burden, lesion eccentricity, microcalcification, large lipid arc, ruptured plaque, and the presence of TCFA; 4) post-PCI CK-MB elevation was observed more frequently in the attenuated group; and 5) EA lesions noted on IVUS and the presence of ruptured plaques on OCT were independent predictors of post-PCI CK-MB elevation in patients treated with elective stenting.

Table 3. Intravascular Ultrasound Findings

	Attenuated Group (n = 47)	Nonattenuated Group (n = 88)	p Value
Lesion EEM CSA, mm^2	18.9 ± 5.9	14.2 ± 5.3	<0.001
Lesion lumen CSA, mm^2	2.24 ± 0.65	2.25 ± 0.64	0.97
Lesion plaque area, mm^2	16.7 ± 5.7	11.9 ± 5.2	<0.001
Lesion plaque burden, %	87.4 ± 4.1	82.7 ± 6.4	<0.001
Reference EEM CSA, mm^2	17.9 ± 5.1	14.1 ± 4.3	<0.001
Positive remodeling	26 (55.3)	34 (38.6)	0.094
Remodeling index	1.06 ± 0.19	1.01 ± 0.18	0.097
Eccentricity	37 (78.7)	46 (52.3)	0.005
Lipid-pool	10 (21.3)	10 (11.4)	0.20
Mild calcification	25 (53.2)	26 (29.5)	0.012
Ruptured plaque	7 (14.9)	5 (5.7)	0.11

Values are mean ± SD or n (%).
CSA = cross-sectional area; EEM = external elastic membrane.

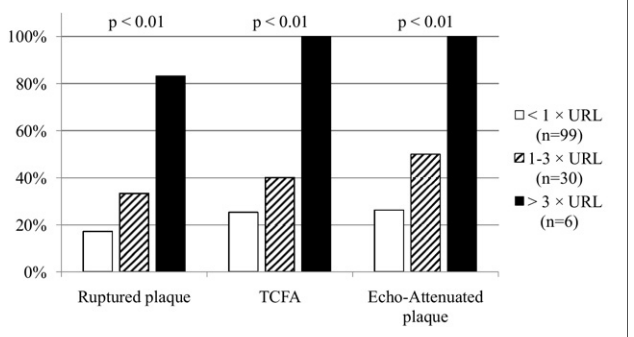

Figure 2. Frequencies of Ruptured Plaques, TCFAs, and EA by Peak CK-MB Category

All of these features increased proportionally to the magnitude of creatine kinase-myocardial band (CK-MB) elevation levels. TCFA = thin-capped fibroatheroma; URL = upper reference limit; other abbreviations as in Figure 1.

We consider that our findings contribute to the understanding of attenuated plaques and their potential relationship to plaque instability. The intensity of the backscattered ultrasound depends on several factors including the ultrasound reflectivity of the tissue. Coronary atherectomy specimens from attenuated plaques show predominantly lipid-rich plaques with microcalcification compared with nonattenuated plaques (4). Irregular distribution of microcalcification and cholesterol clefts and large volumes of these plaque components may cause ultrasound dispersion and signal attenuation behind the plaque (17). Our finding that attenuated plaques are associated with TCFA is in line with these previous observations. TCFA is characterized by macrophage infiltration and a large necrotic core (11,12). A large plaque burden also contributes to EA because of greater distance of ultrasound penetration causing power diminishment in the far field. The presence of TCFA may also cause signal attenuation from the luminal surface because IVUS resolution (100 to 150 μm) cannot detect a thin cap. Thrombi are another potential cause of EA. An animal study suggested that white thrombi might produce greater attenuated ultrasound signal intensity compared with erythrocyte-rich thrombi because white thrombi generally contain more densely homogenous cellular components (18). The previous findings by Lee et al. (5) agree with this observation; they concluded that EA is a finding limited to culprit lesions associated with acute coronary syndrome. In contrast, other reports found EA not only in lesions with acute coronary syndrome but also in SAP (4–6). Our OCT examinations revealed that thrombi might exist in EA lesions, although there was no significant difference in the frequency of thrombi between attenuated and nonattenuated groups. Taken together, our results support the hypothesis that EA is predominantly caused by a combination of factors considered related to plaque instability, such as large vessel size, large plaque burden, eccentricity, microcalcification, plaque rupture, and the presence of TCFA. The present study cohort represents relatively stable patients without pre-PCI CK-MB ele-

Table 4. OCT Findings

	Attenuated Group (n = 47)	Nonattenuated Group (n = 88)	p Value
TCFA	24 (51.1)	19 (21.6)	<0.001
Ruptured plaque	16 (34.0)	16 (18.2)	0.064
Thrombus	6 (12.8)	16 (18.2)	0.47
Lipid-rich plaque	42 (89.4)	49 (55.7)	<0.001
Thinnest cap thickness, μm	60 (50–100)	85 (60–120)	0.005
Lipid quadrants			0.003
0	2 (4.3)	20 (22.7)	
1 (≤90°)	3 (6.4)	19 (21.6)	
2 (>90°, ≤180°)	11 (23.4)	14 (15.9)	
3 (>180°, ≤270°)	16 (34.0)	20 (22.7)	
4 (270°)	15 (31.9)	15 (17.0)	

Values are n (%) or median (25th to 75th percentile).
TCFA = thin-capped fibroatheroma.

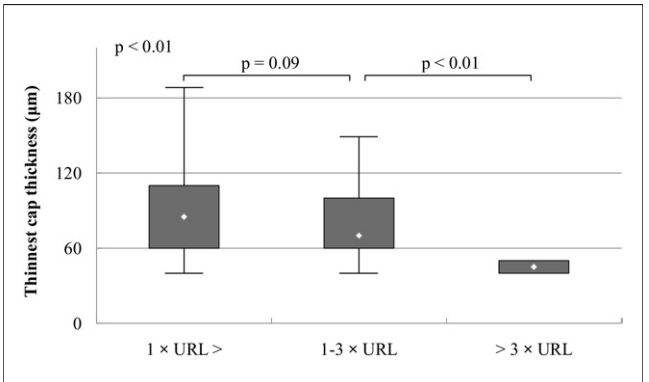

Figure 3. Thinnest Fibrous Cap Thickness by Peak CK-MB Category

Thinnest cap thickness was significantly thinner in the highest CK-MB elevation category than other categories. Abbreviations as in Figure 2.

Table 5. Analysis of Factors Related to CK-MB Elevation After PCI

	Univariate Logistic Regression			Multivariable Logistic Regression		
	p Value	OR	95% CI	p Value	OR	95% CI
RCA	0.041	2.25	1.03–4.89			
ACC/AHA classification B2/C	0.032	2.40	1.08–5.33			
Lesion length	0.043	1.03	1.00–1.06			
QCA RD	0.120	1.70	0.87–3.36			
Attenuated plaque	0.002	8.45	2.22–32.23	0.003	3.49	1.53–7.93
Positive remodeling	0.120	1.84	0.85–3.98			
Lesion EEM CSA	0.032	1.07	1.01–1.14			
Lesion plaque area	0.027	1.08	1.01–1.15			
Reference EEM CSA	0.087	1.07	0.99–1.15			
Lipid-rich plaque	0.037	8.86	1.14–68.66			
TCFA	0.007	2.96	1.34–6.56			
Ruptured plaque	0.004	3.45	1.48–8.01	0.017	2.92	1.21–7.06
Lipid quadrants 3 to 4	0.038	2.30	1.058–5.07			
Cap thickness	0.150	0.99	0.98–1.00			

CI = confidence interval; OR = odds ratio; PCI = percutaneous coronary intervention; QCA = quantitative coronary angiography; TCFA = thin-capped fibroatheroma; other abbreviations as in Tables 1, 2, and 3.

vation. Whether our findings are applicable to EA of the lesions in more unstable patients with acute myocardial infarction remains to be elucidated.

Multivariable analysis demonstrated that EA and the presence of OCT-derived ruptured plaques are independent predictors of post-PCI CK-MB elevation. Severe, acute complications are rare, but a mild and asymptomatic release of the biocardiac markers of myocardial necrosis is frequently observed after an otherwise technically successful coronary intervention. Although the pathophysiology of post-PCI myocardial necrosis is multifactorial, embolization of debris or calcified plaque material, or exposure of thrombogenic material to the coronary flow, which may cause thrombus formation, all seem to play key roles. A recent prospective cohort study by Cavallini et al. (19) reported that the degree of post-PCI CK-MB elevation in patients with normal baseline CK-MB level independently predicted the risk of death after PCI, and even minor increases of CK-MB affected 2-year mortality. Interestingly, an increase in post-PCI troponin I did not affect 2-year mortality and, therefore, added no further prognostic information to that offered by CK-MB elevation. Our study demonstrated that lesions with EA are at high risk for post-PCI myocardial injury; moreover, OCT examination may provide further risk stratification for distal embolization of these high-risk lesions. The relationship between the presence of plaque rupture and potential CK-MB elevation may indicate that the plaques that are most susceptible to distal embolization following PCI also contain the greatest amount of lipid-rich thrombogenic necrotic materials, which may also cause EA. Therefore, we suggest that distal protection devices or other therapeutic approaches may be potentially effective in reducing the release of plaque materials from selective EA lesions in the case of plaque rupture.

Study limitations. First, the present study was a prospective but nonconsecutive series of a relatively small number of subjects who met the eligibility criteria and consented to the study. Excluding patients or lesions, such as patients with significant left main disease, renal impairment, tortuous vessels, or long lesions, may have resulted in a selection bias. Second, the presence of thrombi at the culprit lesion may disturb the accurate assessment of underlying plaque structures by OCT. However, the frequency of thrombi was relatively low in the present study because most of the patients had stable angina. We consider that it is not likely to affect our conclusions. Third, a theoretical possibility of missed CK-MB elevation due to the chosen sampling windows always exists, although we used a widely accepted protocol of periodic CK-MB determination. Fourth, we cannot exclude the possibility that the occlusion or continuous flushing required for OCT imaging, the guidewire, or the OCT imaging wire itself may have altered plaque morphology and the results subsequently obtained by IVUS. Fifth, myocardial necrosis or its location induced by PCI was not confirmed by contrast-enhanced magnetic resonance examinations in the present study. We also recognize the lack of direct comparison of matched lesion sites with and without echo-attenuated plaques in the present study. However, matching individual lesions based on its characteristics may be difficult and impractical due to the possibility of a selection bias. Finally, the present study population represents relatively stable patients with SAP and UAP, and it is not clear if our findings are applicable to patients with acute myocardial infarction.

Conclusions

The present study demonstrates that an echo-attenuated plaque at the culprit lesion was associated with high-risk characteristics. Plaque rupture on OCT examination showed a significant additive predictive value to the presence of EA on IVUS for post-PCI CK-MB elevation.

Reprint requests and correspondence: Dr. Tsunekazu Kakuta, Department of Cardiology, Tsuchiura Kyodo Hospital, 11-7, Manabeshin-machi, Tsuchiura, Ibaraki 300-0053, Japan. E-mail: kaz@joy.email.ne.jp.

REFERENCES

1. Sato H, Iida H, Tanaka A, et al. The decrease of plaque volume during percutaneous coronary intervention has a negative impact on coronary flow in acute myocardial infarction: a major role of percutaneous coronary intervention induced embolization. J Am Coll Cardiol 2004; 44:300–4.
2. Mehran R, Dangas G, Mintz GS, et al. Atherosclerotic plaque burden and CK-MB enzyme elevation after coronary interventions: intravascular ultrasound study of 2256 patients. Circulation 2000;101:604–10.
3. Tanaka A, Kawarabayashi T, Nishibori Y, et al. No-reflow phenomenon and lesion morphology in patients with acute myocardial infarction. Circulation 2002;105:2148–52.
4. Kimura S, Kakuta T, Yonetsu T, et al. Clinical significance of echo signal attenuation on intravascular ultrasound in patients with coronary artery disease. Circ Cardiovasc Interv 2009;2:444–54.
5. Lee SY, Mintz GS, Kim SY, et al. Attenuated plaque detected by intravascular ultrasound: clinical, angiographic, and morphologic features and post-percutaneous coronary intervention complications in patients with acute coronary syndromes. J Am Coll Cardiol Intv 2009;2:65–72.
6. Wu X, Maehara A, Mintz GS, et al. Virtual histology intravascular ultrasound analysis of non-culprit attenuated plaques detected by grayscale intravascular ultrasound in patients with acute coronary syndromes. Am J Cardiol 2010;105:48–53.
7. Mintz GS, Nissen SE, Anderson WD, et al. American College of Cardiology Clinical Expert Consensus Document on Standards for Acquisition, Measurement and Reporting of Intravascular Ultrasound Studies (IVUS): a report of the American College of Cardiology Task Force on Clinical Expert Consensus Documents. J Am Coll Cardiol 2001;37:1478–92.
8. Jang IK, Bouma BE, Kang DH, et al. Visualization of coronary atherosclerotic plaques in patients using optical coherence tomography: comparison with intravascular ultrasound. J Am Coll Cardiol 2002;39: 604–9.
9. Kume T, Akasaka T, Kawamoto T, et al. Assessment of coronary arterial plaque by optical coherence tomography. Am J Cardiol 2006; 97:1172–5.
10. Jang IK, Tearney GJ, MacNeill B, et al. In vivo characterization of coronary atherosclerotic plaque by use of optical coherence tomography. Circulation 2005;111:1551–5.
11. Virmani R, Kolodgie FD, Burke AP, Farb A, Schwartz SM. Lessons from sudden coronary death: a comprehensive morphological classification scheme for atherosclerotic lesions. Arterioscler Thromb Vasc Biol 2000;20:1262–75.
12. Burke AP, Farb A, Malcom GT, Liang YH, Smialek J, Virmani R. Coronary risk factors and plaque morphology in men with coronary disease who died suddenly. N Engl J Med 1997;336:1276–82.
13. The TIMI Study Group. The Thrombolysis In Myocardial Infarction (TIMI) trial. N Engl J Med 1985;312:932–6.
14. Gibson CM, Cannon CP, Daley WL, et al. TIMI frame count: a quantitative method of assessing coronary artery flow. Circulation 1996;93:879–88.
15. Prati F, Cera M, Ramazzotti V, Imola F, Giudice R, Albertucci M. Safety and feasibility of a new non-occlusive technique for facilitated intracoronary optical coherence tomography (OCT) acquisition in various clinical and anatomical scenarios. EuroIntervention 2007;3: 365–70.
16. Yabushita H, Bouma BE, Houser SL, et al. Characterization of human atherosclerosis by optical coherence tomography. Circulation 2002;106: 1640–5.
17. Yamada R, Okura H, Kume T, et al. Histological characteristics of plaque with ultrasound attenuation: a comparison between intravascular ultrasound and histology. J Cardiol 2007;50:223–8.
18. Johnstone E, Friedl SE, Maheshwari A, Abela GS. Distinguishing characteristics of erythrocyte-rich and platelet-rich thrombus by intravascular ultrasound catheter system. J Thromb Thrombolysis 2007;24: 233–9.
19. Cavallini C, Savonitto S, Violini R, et al., for Italian "Atherosclerosis, Thrombosis, and Vascular Biology" and "Society for Invasive Cardiology-GISE" Investigators. Impact of the elevation of biochemical markers of myocardial damage on long-term mortality after percutaneous coronary intervention: results of the CK-MB and PCI study. Eur Heart J 2005;26:1494–8.

Key Words: angioplasty ■ imaging ■ intravascular ultrasound ■ optical coherence tomography.